Science World Journal Vol. 18(No 1) 2023
www.scienceworldjournal.org
ISSN: 1597-6343 (Online), ISSN: 2756-391X (Print)
Published by Faculty of Science, Kaduna State University

Full Length Research Article

THERMAL STABILITY STUDIES BETWEEN NEAT KAOLIN AND IRON (III) OXIDE DOPPED KAOLIN FOR INDUSTRIAL HETEROGENEOUS CATALYSTS DEVELOPMENT

*[1]Abubakar Sani Yelwa; [2]Alhassan Mansur, [3]Lawal Ibrahim Sherifat; [1]Abdulraheem Rofiat and [1]Bello Zainab

[1]Department of Pure and Applied Chemistry; Usmanu Danfodiyo University, P.M.B. 2346, Sokoto, Nigeria
[2]Department of Chemistry, Sokoto State University, P.M.B. 2134, Sokoto, Nigeria
[3]Department of Chemistry College of Preliminary Studies, Yelwa-Yauri P. M. B. 1030, Kebbi State, Nigeria

*Corresponding Author Email Address: abubakar.sani1@udusok.edu.ng Phone: +234 7036154525

ABSTRACT

Thermal stability studies between neat kaolin and iron (iii) oxide (Fe_2O_3/kaolin) dopped kaolin carried out using thermogravimetric analysis (TGA) in order to determine the stability of the two substances over wide temperature ranges. The TGA curves obtained for the two substances analysed revealed four distinct regions of weight loss as the temperature of the analysis keeps rising with time. The percentage weight losses observed for the neat kaolin are 10%, 55%, 20%, 4%, and 2%. Similarly, the percentage weight losses observed for the Fe_2O_3/kaolin are 5%, 30%, 40%, 3%, and 3% respectively. Generally speaking, doping the neat kaolin and its subsequent treatments to produce the Fe_2O_3/kaolin have enhanced the thermal stability of the neat kaolin which is an important property of any given heterogeneous catalyst.

Keywords: *Kaolin, Temperature, Weight, Thermogravimetric, Stability.*

INTRODUCTION:

Catalysis is central to the production of fuels and chemicals, including more than 70% of today's chemical products, thus, the understanding and optimization of heterogeneous catalysts are a critical need within the chemical industry. The considerations put in place when designing a new catalyst or when optimizing the performance of an existing one are activity, selectivity, and durability, thus, a given catalyst must be able to perform a reaction of interest at an acceptable rate under a practical set of temperature and pressure conditions. There is a commercial incentive to tune catalysts to operate at low temperatures and pressures and it is concurrently important that the rate of side reactions are minimal, also, the catalyst must be able to sustain the desired reaction(s) over a long period of time (Bartholomew and Farrauto, 2005; Hagen, 2006).

Catalysts are very important in the chemical industries where they are often used, they can increase the efficiency of a chemical process and minimize the overall cost of manufacturing one or more industrial product(s). Devoting more time and resources to the discovery of new and better catalysts may not be surprising, despite this, the mechanism of action of many catalyzed reactions are not well understood, and many of the catalysts used in the chemical industries were discovered by trial and error rather than by fundamental research (Avey, 1982).

A catalyst is a substance that alters the rate of a chemical reaction, but is not consumed by the reaction; hence, a catalyst can be recovered chemically unchanged at the end of the reaction it has been used to speed up, or catalyze. For chemicals to react, their bonds must be rearranged, because the bonds in the products are different from those in the reactants. The slowest step in the bond rearrangement produces what is termed a transition state. Energy is required to form the transition state, this energy is called the activation energy (Ea). The activation energy can be thought of as a barrier to a chemical reaction, a hurdle that must be crossed and if the barrier is high, few molecules have sufficient kinetic energy to collide, form a transition state, and cross the barrier. Reactants with energy lower than Ea cannot pass through the transition state to react to become the product(s). A catalyst works by providing a different route, with lower Ea, for the reaction(s) to happen. Catalysts lower the energy barrier and the different routes allow the bond rearrangements needed to convert reactants to product(s) to take place more easily, with a lower energy input (Bartholomew and Farrauto, 2005). Most solid catalysts are metals or oxides, sulfides, and halides of metallic elements and of semi-metallic elements like boron, aluminum, and silicon. Gaseous and liquid catalysts are commonly used in their pure form or in combination with suitable carriers or solvents but solid catalysts are commonly dispersed in other substances known as catalyst supports (Bahl *et al* 2000).

Characterization is a central aspect of catalyst development, the elucidation of the structure, composition, and chemical properties of both the solids used in heterogeneous catalysis, the adsorbates and the intermediates present on the surfaces of the catalysts during the reaction is vital for a better understanding of the relationships existing between catalysts properties and the catalytic performance on a wide range of temperature and pressure conditions. This knowledge is essential to the development of a more active, selective, and durable catalyst(s) and also to optimize reaction conditions. The methods commonly used in the characterization of heterogeneous catalysts include chemical analysis, Brunauer-Emmett-Teller (BET) analysis, differential thermal analysis (DTA), thermogravimetric analysis (TGA), Fourier transform infrared spectroscopic (FTIR) analysis, Raman spectroscopic analysis, scanning electron microscopic (SEM) analysis among others (Imelik and Vedrin, 1994).

Thermogravimetric analysis has been extensively used for the characterization of catalysts and clay materials because the method allows for a rapid evaluation of material's changes in response to temperature variations. It is an analytical technique used to determine material's thermal stability and its fraction of volatile components by monitoring the weight change that occurs as the sample is heated over time, the measurement is normally carried out in air or in an inert atmosphere, such as helium or argon, and the weight is recorded as a function of increasing temperature, sometimes, the measurement is performed in a lean oxygen atmosphere (1 to 5% oxygen in nitrogen or helium) to slow down oxidation. In addition to weight changes, some instruments also record the temperature difference between the sample and one or more reference pan (differential thermal analysis, DTA) or the heat flow into the specimen pan compared to that of the reference pan (differential scanning calorimetry, DSC). In particular case of carbon nanotubes, the weight changes in an air is typically a superposition of the weight loss due to oxidation of carbon into gaseous carbon dioxide and the weight gain due to oxidation of residual metal catalyst into metallic oxides (Jean-François, 2018).

MATERIALS AND METHODS:

The laboratory apparatus used in this research are listed on Table 1

Table 1: List of Apparatus

S/No.	Equipment	Model	Manufacturer
1.	Weighing Balance	Adventurer, AR 3130	OHAUS, China.
2.	Thermogravimetric Analyser	DTG 60AH	Lab. Cognition GmbH, Germany
3.	Muffle Furnace	MF 207	NÛVE SANAYI, TURKEY
4.	Ultrsonicator	DR-LQ20	Derui Ltd.
5.	Drying oven	DHG-9023A	Surgifriend Medics, England

Table 2: List of reagents

S/No.	Reagent	% Purity	Manufacturer
1.	$Fe(NO_3)_3.9H_2O$	98.0	Qualikems

Sample collection and treatment

Kaolin sample was collected from a kaolin quarry site in Kankara town of Kankara Local Government area of Katsina State on the geographical coordinates of 11°55’47” N × 7°25’11” E following the literature methods (Atta *et al.,* 2007; Jide, 2014 and Hadi *et al.,* 2016)

~~A~~ clean shovel was used to dig a v-shaped hole of 20 cm depth at each sampling point then a slice of the kaolin was taken and stored in a clean glass bottle, eight sub-samples (100g) each per hectare were taken to form one composite sample and the depth at which the sub-samples were taken range from 2 to 20 cm. The composite samples were inserted into clean glass containers each and labelled as A1, A2, A3, A4, A5, A6, A7, and A8 respectively, after which, they were transported to the laboratory. In the laboratory, each composite sample was grounded using a pestle and mortar. The samples were further combined to form one homogeneous composite sample that was subjected to a series of cone and quartering methods to obtain a representative sample of 200 mg that was pulverized again and then sieved through 2 mm mesh sieve. The pulverized kaolin (100 g) was transferred into a 1000 cm^3 beaker containing 400 cm^3 distilled water and the mixture was stirred and allowed to stand for 1 hr after which it was decanted. The washing was repeated two more times to remove suspended particles from the kaolin and the wet kaolin was oven dried at 105 ^oC for 12 hours~~,~~ the dried kaolin was pulverized, sieved, and then stored in a clean glass container for use.

Preparation of reagent

The 0.1252 M $Fe(NO_3)_3\bullet 9H_2O$ used to prepare 20 wt% Fe_2O_3/kaolin was prepared as follows:

50.5989 g of $Fe(NO_3)_3\bullet 9H_2O$ salt was dissolved into a 500 cm^3 beaker containing 200 cm^3 of distilled water. The mixture was stirred until the salt dissolved and the solution was transferred into a 1000 cm^3 volumetric flask, the beaker was washed two more times with distilled water and the washings were transferred into the volumetric flask containing the solution and the volume of the solution was adjusted to 1000 cm^3 using distilled water.

Preparation of iron (iii) oxide on kaolin (Fe_2O_3/kaolin)

The metal oxide on kaolin prepared was prepared by impregnation method as follows:

100 g of the neat kaolin was transferred into a 1000 cm^3 beaker and 300 cm^3 of the prepared 0.1252 M solution of $Fe(NO_3)_3\bullet 9H_2O$ was added to it and the mixture was stirred for 30 min, it was then ultrasonicated for 8 hrs. at 80 ^0C after which it was allowed to age for 24 hr. After aging, the mixture was placed on a hot plate at 80 ^oC to evaporate the excess solvent, after which it was oven dried at 105 ^oC for 24 hrs. The dried mass was pulverized using a pestle and mortar and then sieved through a 2 mm mesh sieve.

The dried mixture of Iron (iii) nitrate nonahydrate and kaolin was then subjected to calcination. During the calcination process a given mass of the iron (iii) nitrate nonahydrate treated kaolin was weighed in a crucible and the crucible and its contents were inserted into a muffle furnace that was set at 320 ^oC and the calcination was carried out for 2 hrs. The calcination product (Fe_2O_3/kaolin) was allowed to cool to room temperature and then it was removed from the muffle furnace and the material was taken for thermogravimetric analysis, however, the neat kaolin was not subjected to the above treatment, rather, it was only subjected to the thermogravimetric analysis under the same condition with the iron (iii) nitrate nonahydrate treated kaolin (Fe_2O_3/kaolin). The decomposition of $Fe(NO_3)_3\bullet 9H_2O$ during calcination is given by Eq. 1

$$4Fe(NO_3)_3\bullet 9H_2O \longrightarrow 2Fe_2O_{3(S)} + 12NO_{2(g)} + 9H_2O_{(g)} + 3O_{2(g)} \quad \ldots\ldots 1$$

The thermogravimetric analysis of both the neat kaolin and the Fe_2O_3/kaolin was conducted at a heating rate of 10 °C/min under a nitrogen atmosphere (99.99%, 20 mL/min). Each sample was pretreated with nitrogen at 383 K for 1hr and 12.226 mg of each sample was introduced into the sample holder of the machine and the analysis was conducted at a heating rate of 10 ^oC per minute over a temperature range of 30 to 950 ^oC for 2 hrs. The TGA curves observed for both the neat kaolin and the Fe_2O_3/kaolin are displayed Figure 1 and Figure 2 respectively.

Results

The TGA curves for the neat kaolin and the Fe_2O_3/kaolin are displayed **in** Figure 1 and Figure 2 respectively.

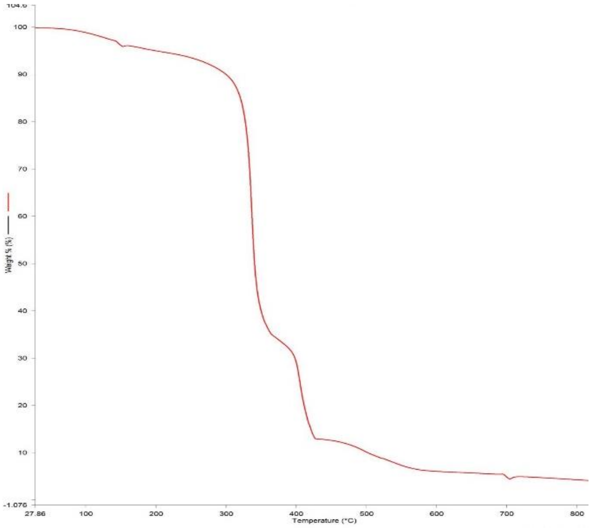

Figure 1.: TGA curve of neat kaolin

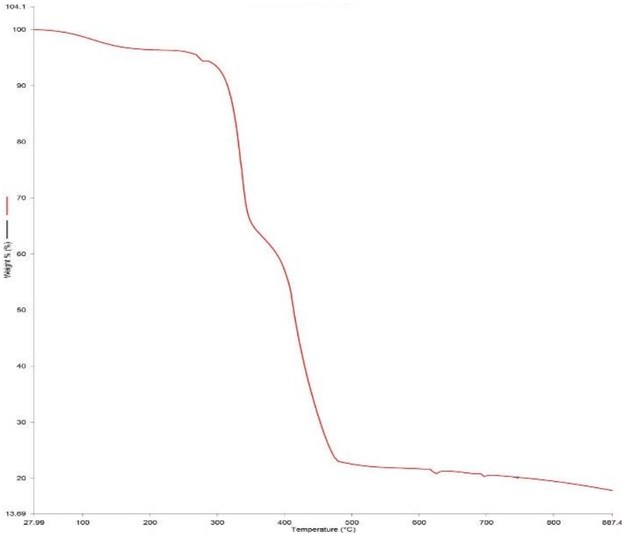

Figure 2.: TGA curve of Fe_2O_3/kaolin

DISCUSSION

Figure 1 is the TGA curve of the neat kaolin showing four distinct changes during the thermal analysis. At the onset of the thermogravimetric (TG) analysis of the neat kaolin there was a lean weight loss of the sample resulting in a gentle slope of the TGA curve from a temperature of 27 to 300 °C and the percentage weight loss observed at this step was 10%. This weight loss is associated with dehydration and volatalisation of hydration waters been adhessesd to the neat kaolin. The second step of the thermal analysis of the neat kaolin shows a steep slope of the curve from a temperature of 301 to 380 °C and the percentage weight loss observed at this step was 55%. The high loss in mass observed at this step is associated to the loss of physiosorbed and interlayer waters. The third step of the thermal analysis of the neat kaolin commenced from a temperature of 381 to 420 °C, also this step shows a steep slope of the TG curve and the percentage weight loss observed here was 20% and the loss in mass is attributed to the loss of interlayer hydroxyl groups and dihydroxylation of structural and coordinated waters usually at temperatures above 400 °C. The fourth step of the weight loss of the neat kaolin commenced from a temperature of 421 to 852 °C. This step shows a gradual slope of the TGA curve and the percentage weight loss observed was 15%. The weight loss observed at this step is attributed to the dehydroxylation of kaolinite and the decomposition of Al and Fe hydroxides (Panda *et al.,* 2010; San CristÒbal *et al.,* 2009; Mohsen and El-Maghraby, 2010). The loss of physisorbed and interlayer waters and the dehydroxylation of structural and coordinated waters leading to the transformation of kaolinite to metakaolinite are usually observed at temperature above 650 ^{o}C (Kumar *et al.,* 2013).

Similarly, the thermal analysis of the Fe_2O_3/kaolin shows four distinct regions of the TGA curve but having slight differences in the percentage losses of weight as compared to the TGA curve of the neat kaolin. The first step of the thermal analysis of the Fe_2O_3/kaolin begins from a temperature of 27 ^{o}C to 280 ^{o}C and the weight loss observed at this was 5% as against 10% observed for the neat kaolin and as well the TG curve was observed to display a gradual slope similar to the curve displayed at the first step of the thermal analysis of the neat kaolin. This weight loss is attributed to the loss of hydration and physisorbed waters (Sietsma *et al.,* 2008). The second step of the TGA curve of the Fe_2O_3/kaolin commenced from a temperature of 281 to 350 ^{o}C and the weight loss observed here was 25% as against 55% observed for the neat kaolin, however, the TG curve was observed to have a very steep slope similar to the steep slope at the second step of the thermal analysis of the neat kalolin. The loss in mass observed at this step is attributed to the loss of the water molecules in the first coordination sphere of the interlayer ions (Kumar *et al.,* 2013). The third step of the thermal analysis commenced from a temperature of 351 to 480 ^{o}C and the observed loss in mass at this step was 50% as against 20% observed for the neat kaolin. Also, the TGA curve displayed a similar steep slope as the third step of the third step of the thermal analysis of the neat kaolin and the change observed here is associated with the loss of structural hydroxyl groups that usually condense and dehydrate at temperature range of 500-800 °C. The fourth step of the thermal analysis of Fe_2O_3/kaolin commenced from a temperature of 481 to 880 °C displaying a gentle slope of the curve and the loss in mass observed at this step was 20% as against 15% observed for the neat kaolin and the loss in mass observed at this step is associated with the dehydroxylation and loss of coordinated waters within the kaolinite structure.

Generally speaking, the two curves for the thermal analysis of the neat kaolin and that of the Fe_2O_3/kaolin were observed to follow a similar pattern of weight losses as the temperature of the analysss of the two materials keeps rising from a room temperature to a temperature of over 800 °C. Therefore, the differences in weight losses observed between the two materials (neat kaolin and Fe_2O_3/kaolin) is attributed to the doping some quantities of the neat kaolin with iron (iii) trioxonitrate (v) and its subsequent calcination at temperature of 320 °C for 2 hrs. to produce the Fe_2O_3/kaolin. However, the first steps of the thermal analysis of the neat kaolin and that of the Fe_2O_3/kaolin shows a similar gentle slope for the two materials over a similar temperature range of 27 to 300 °C for the former and 27 to 280 °C for the later. Similarly, the second steps of the TGA curves of both the materials show a steep slope each over temperature ranges of 301 to 380 °C for the former and 281 to 350 ^{o}C for the later material, however, the second step of the TGA curve displayed by the neat kaolin was observed to show a steeper and a longer range of the curve than the second step of the TGA curve of Fe_2O_3/kaolin. In a reverse scenario, the third step of the TGA curve displayed by the neat kaolin shows a steep slope of the curve within the temperature range of 381 to 420 °C but a shorter range of the curve was observed when compared to the third step of the curve displayed by Fe_2O_3/kaolin which shows a steeper and a longer range of the curve on a temperature range of 351 to 480 ^{o}C. The fourth step of the TGA curve of the neat kaolin displayed a gentle slope of the curve over a temperature range of 421 to 852 °C and similarly, the fourth step of the TGA curve of Fe_2O_3/kaolin displayed a gentle slope over a temperature range of 481 to 880 °C.

Therefore, the first to the fourth steps of the TGA curves for both the neat kaolin and Fe_2O_3/kaolin displayed strong similarities particularly at the first and fourth steps of the thermal analysis in which both steps show a gentle slope of the curves. In a reverse scenario, the second steps of the TGA curves of both the neat kaolin and Fe_2O_3/kaolin displayed a steep slope of the curve, however, the second step of the curve of the former was observed to be much steeper and having a longer range of than the second step of the TGA curve of the later. This differential in the curve shapes observed at the second step of each substance is attributed to the effect of doping the neat kaolin to form the Fe_2O_3/kaolin. Similarly, the third step of the TGA curves of both the neat kaolin and Fe_2O_3/kaolin displayed an opposite scenario to the second steps of the thermal analysis. In this step the TGA curve of the former was observed to be less steep and shorter than the curve of the later. The differences in the curve shapes observed here is dominantly due to the resistance of the dopped kaolin to undergo weight loss associated with the loss of the interlayer hydroxyl groups and dehydroxylation of structural and coordinated waters at elevated temperatures. Therefore, generally speaking doping the neat kaolin and its subsequent treatments to produce the Fe_2O_3/kaolin have enhanced the thermal stability of the neat kaolin which is an important property of any given heterogeneous catalyst.

REFERENCES

Avey, H. E., (1982). Basic Reaction Kinetics and Mechanisms. Hong Kong: The Macmillan Press Ltd. p. 113 8 .

Bahl, A. B. S., and Tuli, G. D., (2000). Essentials of Physical Chemistry, New Delhi: S. Chand and Company Ltd. p. 706 8 .

Bartholomew, C. H., and Farrauto, R. J., (2005). Fundamentals of Industrial Catalytic Processes, 2nd ed., Wiley-Aiche, New York.

Hadi, B., Muhammad, A. S., Garba, M. M., and Muhammad, A. B., (2016). Effect of Neat Kaolin and CuO/Kaolin on the Yield and Composition of Products of Pyrolysis of Polystyrene Waste. *Journal of Taylor and Francis Group* **0** (0) p. 6

Atta, A. Y., Ajayi, O. A., and Adefila, S. S. (2007). Synthesis of Faujasite Zeolites from Kankara Kaolin clay. *J. Appl. Sci. Res*. 3:1017–1021. [Google Scholar]

Jide, A. (2014). Characterisation of the Nigerian Kankara Kaolinite clay particulates for automobile friction lining material development. *Chem. Process Eng. Res*. 29:24–34. [Google Scholar]

Hagen, J., (2006). Industrial Catalysis: A Practical Approach, Wiley-VCH, Weinheim, Germany. p. 8

Imelik, B., and Jacques, C. V., (1994). Catalyst Characterization Physical Techniques for Solid Materials: Springer Science Business Media New York Originally published by Plenum Press, New York in 1994.

Jean-François, L., (2018). Developments in Clay Science, Volume 9, pp. 195-253.

Kumar, S., Panda, A. K., and Singh, R. K., (2013). Preparation and Characterisation Acids and Alkalis Treated Kaolin Clay. *Bulletin of Chemical Reaction Engineering and Catalysis*. **8** (1) p. 66

Mohsen, Q., and El-Maghraby, A., (2010). Characterisation and Assessment of Saudi Clays Raw Materials at Different Area. *Arabian Journal of Chemistry* **3** (1) p. 271.

Panda, A. K., Mishra, B. G., Mishra, D. K., and Singh, R. K., (2010). Effect of Sulphuric Acid Treatment on the Physico-Chemical Characteristics of Kaolin Clay. Journal of Colloid and Surfaces A: Physicochemical Engineering Aspect, **363** (9) p. 101.

San CristÒbal, A. G., Castello, R., Luengo, M. A. M., and Vizcayno, C., (2009). Acid Activation of Thermally and Mechanically Modified Kaolins. *Journal of Materials Research Bulletin,* **7** (44) p. 2107

Sietsma, J., R., A., Meeldijk, J., D., den Breejen, J., P., Versluijs-Helder, M., van Dillen, A., J., de Jongh, P., E., and de Jong, K., P., (2007). The Preparation of Supported NiO and Co_3O_4 Nanoparticles by the Nitric Oxide Controlled Thermal Decomposition of Nitrates. Angew Chem. Int. ed. 46: p. 3.